High Dynamic Range Imaging by Perceptual Logarithmic Exposure Merging

Corneliu Florea CORNELIU.FLOREA@UPB.RO
Image Processing and Analysis Laboratory
University "Politehnica" of Bucharest, Romania, Address Splaiul Independenţei 313

Constantin Vertan CONSTANTIN.VERTAN@UPB.RO
Image Processing and Analysis Laboratory
University "Politehnica" of Bucharest, Romania, Address Splaiul Independenţei 313

Laura Florea LAURA.FLOREA@UPB.RO
Image Processing and Analysis Laboratory
University "Politehnica" of Bucharest, Romania, Address Splaiul Independenţei 313

Abstract

In this paper we point out to a similarity between Logarithmic-Type Image Processing (LTIP) model and the Naka-Rushton model of the Human Visual System (HVS). LTIP is a derivation of the Logarithmic Image Processing (LIP), which further replaces the logarithmic function with a ratio of polynomial functions. Based on this similarity, we show that it is possible to present an unifying framework to the High Dynamic Range (HDR) imaging problem, namely that performing exposure merging under the LTIP model is equivalent to standard irradiance map fusion. The resulting HDR algorithm is shown to provide high quality in both subjective and objective evaluations.

1. Introduction

Motivated by the limitation of the digital camera towards real scenes with large lightness dynamic range, a category of image acquisition and processing techniques, collectively named High Dynamic Range (HDR) Imaging, gained popularity. To acquire HDR scenes, consecutive frames with different exposures are typically acquired and combined into a HDR image that is viewable on regular displays and printers.

In parallel, Logarithmic Image Processing (LIP) models were introduced as an alternative to image processing with real based operations. While initially modelled from the cascade of two transmitting filters (Jourlin and Pinoli, 1987), later it was showed that the LIP models can be generated by the homomorphic theory and they do have a cone space structure (Deng et al., 1995). The initial model was showed to be compatible with Weber-Fechner perception law (Pinoli and Debayle, 2007), which is not unanimously accepted (Stevens, 1961). Currently, most global Human Visual Systems (HVS) models are extracted from the Naka-Rushton equation of photoreceptor absorption of incident energy and are followed by further modelling of the local adaptation. We will show here that the new LIP extension model introduced in (Vertan et al., 2008) (which no longer uses a logarithmic generative function but only a logarithmic-like function) is consistent with the global human perception as described by the Naka-Rushton model. In such a case, the generative function of the LTIP model transfers the radiometric energy domain into human eye compatible image domain, thus mimicking by itself and its inverse both the camera response function and the human eye lightness perception.

The current paper claims three contributions: First, we show that the previously introduced LTIP model is compatible with Naka-Rushton/Michaelis-Menten model of the eye global perception. Secondly, based on the previous finding, we show that it is possible to treat two contrasting HDR approaches unitary if the LTIP model framework is assumed. Thirdly, the reinterpretation of the exposure merging algorithm (Mertens et al., 2007) under the LTIP model produces a new algorithm that leads to qualitative results.

The remainder of the paper is constructed as follows: in section 2 we present a short overview of the existing HDR trends and we emphasize their correspondence with human perception. In section 3, state of the art results in the LIP framework and the usage of the newly introduced LTIP framework for the generation of models compatible with human perception are discussed. In section 4 we derive and motivate the submitted HDR imaging, such that in section 5 we discuss implementation details and achieved results, ending the paper with discussion and conclusions.

2. Related work

The typical acquisition of a **High Dynamic Range** image relies on the "Wyckoff Principle", that is differently exposed images of the same scene capture different information due to the differences in exposure (Mann and Picard, 1995). Bracketing techniques are practically used to acquire pictures of the same subject but with consecutive exposure values. These pictures are then fused to create the HDR image.

For the fusion step two directions were assumed. The first direction, named irradiance fusion, acknowledged that the camera recorded frames are non-linearly related to scene reflectance and, thus, it relied on the irradiance maps retrieval from the acquired frames, by inverting the camera response function (CRF), followed by fusion in the irradiance domain. The fused irradiance map is compressed via a tone mapping operator (TMO), into a displayable low dynamic range image. The second direction, called exposure fusion, aimed at simplicity and directly combined the acquired frames into the final image. A short comparison between these two is presented in table 1 and detailed in further paragraphs.

2.1. Irradiance fusion

Originating in the work of (Debevec and Malik, 1997), the schematic of the irradiance fusion may be followed in figure 1 (a). Many approaches were schemed for determining the CRF (Grossberg and Nayar, 2004). We note that the dominant shape is that of a gamma function (Mann and Mann, 2001), trait required by the compatibility with the HVS.

After reverting the CRF, the irradiance maps are combined, typically by a convex combination (Debevec and Malik, 1997), (Robertson et al., 1999). For proper displaying, a tone mapping operator (TMO) is then applied on the HDR irradiance map to ensure that in the compression process all image details are preserved. For this last step, following Ward's philosophy (Ward et al., 1997), typical approaches adopt a psychovisual-inspired function for domain compression, followed by local contrast enhancement. For a survey of the TMOs we refer to the paper of (Ferradans et al., 2012) and to the book by (Banterle et al., 2011).

Among other TMO attempts, a notable one was proposed by (Reinhard et al., 2002) which, inspired by Ansel Adams' Zone System, first applied a logarithmic scaling to mimic the exposure setting of the camera, followed by dodging-and-burning for the actual compression. (Durand and Dorsey, 2002) separated, by means of a bilateral filter, the HDR irradiance map into a base layer that encoded large scale variations (thus, needing range compression) and into a detail preserving layer to form an approximation of the image pyramid. (Fattal et al., 2012) attenuated the magnitude of large gradients based on a Poisson equation. (Drago et al., 2003) implemented a logarithmic compression of luminance values that matches the HVS. (Krawczyk et al., 2005) implemented the gestalt based anchoring theory of (Gilchrist et al., 1999) to divide the image in frameworks and performed range compression by ensuring that frameworks are well-preserved. (Banterle et al., 2012) segmented the image into luminance components and applied independently the TMOs introduced in (Drago et al., 2003) and in (Reinhard et al., 2005) for further adaptive fusion based on previously found areas. (Ferradans et al., 2012) proffered an elaborated model of the global HVS response and pursuit local adaptation with an iterative variational algorithm.

Yet, as irradiance maps are altered with respect to the reality by the camera optical systems, additional constraints are required for perfect matching with the HVS. Hence, this category of methods, while being theoretically closer to the pure perceptual approach, requires supplementary and costly constraints and significant computational resources for the CRF estimation and for the TMO implementation.

2.2. Exposure merging

Noting the high computational cost of the irradiance maps fusion, (Mertens et al., 2007) proposed to implement the fusion directly in the image domain; this approach is described in figure 1 (b). The method was further improved for robustness to ghosting artifacts and details preservation in HDR composition by (Pece and Kautz, 2010).

While being sensibly faster, the exposure fusion is not physically based, nor perceptually inspired. However, while the academic world tends to favor perceptual approaches as they lead to images that are correct from a perceptual point of view, the consumer world naturally tends to favor images that are photographically more spectacular and the exposure merging solution pursuits this direction.

Table 1. Comparison of the two main approaches to the HDR problem.

Method	CRF recovery	Fused Components	Fusion Method	Perceptual
Irradiance fusion (Debevec and Malik, 1997)	Yes	Irradiance Maps	Weighted convex combination	Yes (via TMO)
Exposure fusion (Mertens et al., 2007)	No	Acquired Frames	Weighted convex combination	No

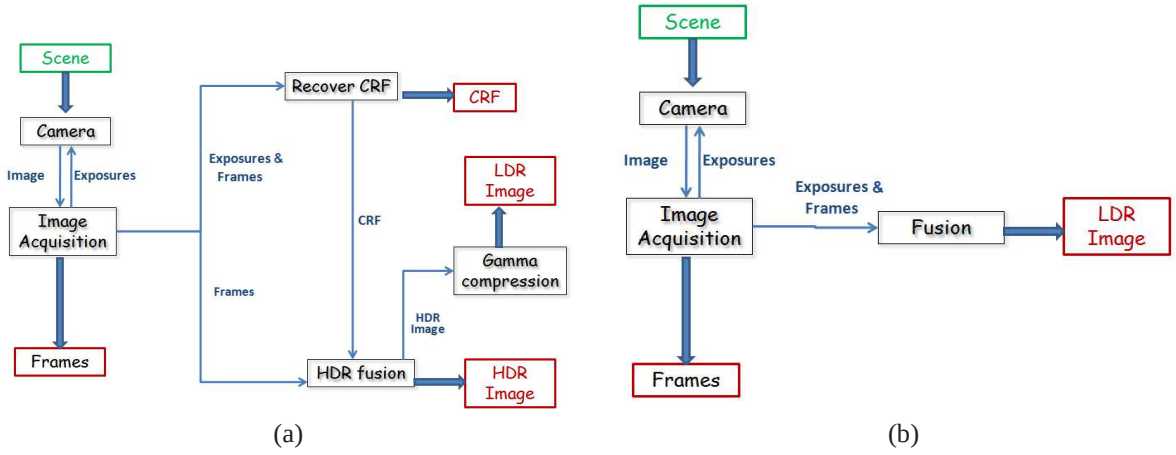

Figure 1. HDR imaging techniques: (a) irradiance maps fusion and (b) exposure fusion. Irradiance map fusion relies on inverting the Camera Response Function (CRF) in order to return into the irradiance domain, while the exposure fusion works directly in the image domain, and thus avoiding the CRF reversal.

3. Logarithmic Type Image Processing

Typically, image processing operations are performed using real-based algebra forming the so-called Classical Linear Image Processing, which proves its limitations under specific circumstances, like upper range overflow. To negotiate with such situations, non-linear image processing methods have been developed (Rafajlowicz et al., 2005). Such examples are the LIP models. The first LIP model was constructed by Jourlin and Pinoli (Jourlin and Pinoli, 1987) starting from the equation of light passing through transmitting filters.

The LIP model was further developed into a robust mathematical structure, namely a cone/vector space. Subsequently many practical applications have been presented and an extensive review of advances and applications for the classical LIP model is presented in (Pinoli and Debayle, 2007). In parallel, other logarithmic models and logarithmic-like models were reported. In this particular work we are mainly interested in the logarithmic-like model introduced by (Vertan et al., 2008), which has a cone space structure and is named LTIP model. A summary of existing models may be followed in (Navarro et al., 2013). Recently parametric extensions of the LTIP models were also introduced (Panetta et al., 2011), (Florea and Florea, 2013). The original LIP and the LTIP models as well as the general parametric extension are summarized in table 2.

3.1. Relation between LIP models and HVS

From its introduction in the 80s, the original LIP model had a strong argument being similar with the Weber-Fechner law of contrast perception. This similarity was thoroughly discussed in (Pinoli and Debayle, 2007), where it was showed that logarithmic subtraction models the increment of sensation caused by the increment of light with the quantity existing in the subtraction. Yet the logarithmic model of the global perceived luminance contrast system assumed by the Weber-Fechner model was vigorously challenged (Stevens, 1961) and arguments hinted to the power-law rules (Stevens and Stevens, 1963). Thus, we note that the Stevens model is more inline with the LTIP model. On the other hand, Stevens experiments were also questioned (Macmillan and Creelman, 2005), so it does not seem to be a definite answer in this regard.

Still, in the latest period, evidence seems to favor the Naka-Rushton/Michaelis-Menten model of retinal adaptation (Ferradans et al., 2012), thus an important class of TMO techniques following this model for the global adaptation step. The Naka-Rushton equation is a particular case of the Michaelis-Menten model that expresses the hyperbolic relationship between the initial velocity and the substrate concentration in a number of enzyme-catalyzed

Table 2. The classical LIP model introduced by Jourlin and Pinolli (LIP), the logarithmic type (LTIP) model with the basic operations and the parametric extension of the LTIP model. D is the upper bound of the image definition set (typically $D = 255$ for `unsigned int` representation or $D = 1$ for `float` image representation).

Model	Domain	Isomorphism	Addition $u \oplus v$	Scalar multiplication $\alpha \otimes u$
LIP	$\mathcal{D}_\phi = (-\infty; D]$	$\Phi(x) = -D \log \frac{D}{D-x}$	$u + v + \frac{uv}{D}$	$D - D\left(1 - \frac{u}{D}\right)^\alpha$
LTIP	$\mathcal{D}_\phi = [0; 1)$	$\Phi(x) = \frac{x}{1-x}$	$1 - \frac{(1-u)(1-v)}{1-uv}$	$\frac{\alpha u}{1+(\alpha-1)u}$
Parametric LTIP	$\mathcal{D}_\phi = [0; 1)$	$\Phi_m(x) = \frac{x^m}{1-x^m}$	$\sqrt[m]{1 - \frac{(1-u^m)(1-v^m)}{1-u^m v^m}}$	$u \sqrt[m]{\frac{\alpha}{1+(\alpha-1)u^m}}$

reactions. Such a process is the change of the electric potential of a photoreceptor (e.g. the eye cones) membrane, $r(\mathcal{I})$ due to the absorption of light of intensity $\mathcal{I}$. The generic form, called Michaelis-Menten equation (Valeton and van Norren, 1983)is:

$$r(\mathcal{I}) = \frac{\Delta V(\mathcal{I})}{\Delta V_{\max}} = \frac{\mathcal{I}^n}{\mathcal{I}^n + \mathcal{I}_S^n} \tag{1}$$

where $\Delta V_{\max}$ is the maximum difference of potential that can be generated, $\mathcal{I}_S^n$ is the light level at which the photoreceptor response is half maximal (semisaturation level) and n is a constant. (Valeton and van Norren, 1983) determine that $n = 0.74$ for rhesus monkey. If $n = 1$ the Naka-Rushton equation (Naka and Rushton, 1966) is retrieved as particular case of the Michaelis-Menten model:

$$r(\mathcal{I}) = \frac{\Delta V(\mathcal{I})}{\Delta V_{\max}} = \frac{\mathcal{I}}{\mathcal{I} + \mathcal{I}_S} \tag{2}$$

For the TMO application, it is considered that the electric voltage in the right is a good approximation of the perceived brightness (Ferradans et al., 2012). Also, it is not uncommon (Meylan et al., 2007) to depart from the initial meaning of semisaturation for $\mathcal{I}_S$ (the average light reaching the light field) and to replace it with a convenient chosen constant. TMOs that aimed to mimic the Naka-Rushton model (Reinhard et al., 2002), (Tamburino et al., 2008) assumed that the HDR map input was $\mathcal{I}$ and obtained the output as $r(\mathcal{I})$.

On the other hand, the generative function of LIP models maps the image domain onto the real number set. The inverse function acts as a homomorphism between the real number set and the closed space that defines the domain of LIP. For the logarithmic-like model, the generative function is $\Phi_V(x) = \frac{x}{1-x}$ while the inverse is: $\Phi_V^{-1}(y) = \frac{y}{y+1}$.

$$\Phi_V^{-1}(y) = \frac{y}{y+1} \tag{3}$$

The inverse function (eq. (3)) mimics the Naka-Rushton model (eq. 2) with the difference that instead of the semi-saturation, $\mathcal{I}_S$, as in the original model, it uses full saturation. Given this observation, we interpreted logarithmic-like model as the mapping of the irradiance intensity (which are defined over the real number set) onto photoreceptor acquired intensities, i.e human observable chromatic intensity. While the logarithmic-like model is only similar and not identical with the Naka-Rushton model of the human eye, it has the strong advantage of creating a rigorous mathematical framework of a cone space.

3.2. Relation between the LIP models and CRF

The dominant non-linear transformation in the camera pipe-line is the gamma adjustment necessary to adapt the image to the non-linearity of the display and respectively of the human eye. The entire pipeline is described by the Camera Response Function (CRF) which, typically, has a gamma shape (Grossberg and Nayar, 2004). While analytical models were regressed from actual data (Mann and Mann, 2001), (Mitsunaga and Nayar, 1999), they don't perfectly fit.

It was previously pointed to the similarity between the the LTIP generative function and the CRF (Florea and Florea, 2013). To show the actual relation between the LTIP generative function and the CRF, we considered the DoRF database (Grossberg and Nayar, 2004) which consists of 200 recorded response functions of digital still cameras and analogue photographic films. These functions are showed in figure 2 (a); to emphasize the relation, in subplot (b) of the same figure we represented only the LTIP generative function and the average CRF. As one may see, while the LTIP generative function is not identical to the average CRF, there do exist camera and films that have a response function identical to the LTIP generative function.

4. HDR by Perceptual Exposure Merging

Once that camera response function, g, had been found, the acquired images f_i are turned into irradiance maps, E_i by (Debevec and Malik, 1997):

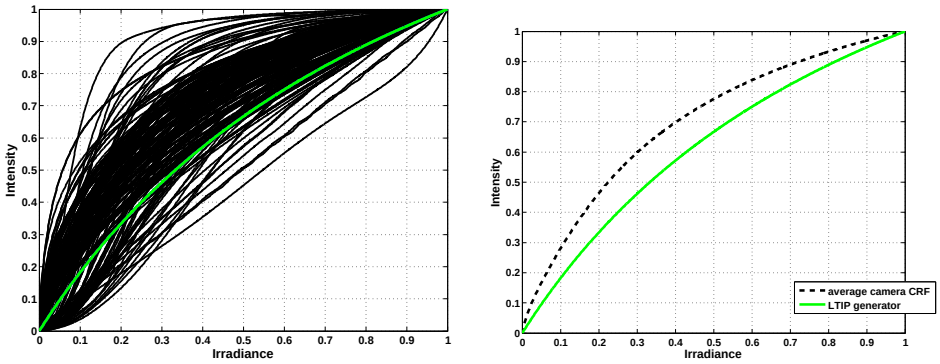

(a) (b)

Figure 2. The relation between the LTIP generative function Φ_V and camera response functions as recorded in DoRF database: (a) full database and (b) average CRF (black) with respect to the LTIP function (green).

$$E_i(k,l) = \frac{g^{-1}\left(f_i(k,l)\right)}{\Delta t} \tag{4}$$

where Δt is the exposure time and each pixel location, (k,l) is computed independently. Further, the HDR irradiance map is calculated as the weighted sum of the acquired irradiance maps (Debevec and Malik, 1997), (Robertson et al., 1999):

$$E_{HDR}(k,l) = \frac{\sum_{i=1}^{N} \mu\left(f_i(k,l)\right) \cdot E_i(k,l)}{\sum_{i=1}^{N} \mu\left(f_i(k,l)\right)} \tag{5}$$

where $\mu\left(f_i(k,l)\right)$ are weights depending on the chosen algorithm.

However, we stress that the weights are scalars with respect to image values. This means that their sum is also a scalar and we denote it by:

$$\eta = \sum_{i=1}^{N} \mu\left(f_i(k,l)\right) \tag{6}$$

Taking into account that the CRF may be approximated by the LTIP generative function g and, also, that the final image was achieved by a tone mapping operator from the HDR irradiance map, we may write that:

$$f_{HDR}(k,l) = g\left(E_{HDR}(k,l)\right) \tag{7}$$

If one expands the HDR irradiance map using eq. (5), he will obtain:

$$\begin{aligned} f_{HDR}(k,l) &= g\left(\tfrac{1}{\eta}\textstyle\sum_{i=1}^{N} \mu\left(f_i(k,l)\right) \cdot E_i(k,l)\right) \\ &= \tfrac{1}{\eta} \otimes g\left(\textstyle\sum_{i=1}^{N} \mu\left(f_i(k,l)\right) \cdot E_i(k,l)\right) \\ &= \tfrac{1}{\eta} \otimes \left(\oplus \textstyle\sum_{i=1}^{N} g\left(\mu\left(f_i(k,l)\right) \cdot E_i(k,l)\right)\right) \\ &= \tfrac{1}{\eta} \otimes \left(\oplus \textstyle\sum_{i=1}^{N} \left(\mu\left(f(k,l)\right)\right) \otimes g\left(E_i(k,l)\right)\right) \\ &= \tfrac{1}{\eta} \otimes \left(\oplus \textstyle\sum_{i=1}^{N} \left(\mu\left(f_i(k,l)\right)\right) \otimes f_i(k,l)\right) \end{aligned} \tag{8}$$

where $\otimes$ and $\oplus$ are the LTIP operations showed in table 2, while $\left(\oplus \sum_{i=1}^{N} u_i\right)$ stands for:

$$\left(\oplus \sum_{i=1}^{N} u_i\right) = u_1 \oplus u_2 \oplus \cdots \oplus u_N$$

Eq. (8) shows that one may avoid the conversion of the input images to irradiance maps, as the HDR image may be simply computed using addition and scalar multiplications in the logarithmic domain. Furthermore, we have to point out, that while we have started our calculus based on the irradiance maps fusion, eq. (8), if written with real-based operations, it matches the exposure fusion introduced in (Mertens et al., 2007). Thus, the use of the LTIP operations creates a unifying framework for both approaches. In parallel, it adds partial psychovisual support for the exposure fusion variant.

Regarding the weights, $\mu\left(f(k,l)\right)$, they should complement the global tone mapping by performing local adaptation. In (Mann and Mann, 2001) these weights are determined by derivation of the CRF, while in (Mertens et al., 2007) they are extracted as to properly encode contrast, saturation and well-exposedness. More precisely:

- *contrast*, w_C is determined by considering the response of Laplacian operators; this is a measure of the local contrast which exists in human perception as center-surround ganglion field organization.

- *saturation*, w_S is computed as the standard deviation of the R, G and B values, at each pixel location. This component favors photographic effects since the normal consumers are more attracted to vivid images and has no straight-forward correspondence to human perception.

- *well-exposedness* w_e is computed by giving small weights to values in the mid-range and large weights to outliers favoring the glistening aspect of consumer approaches. More precisely, one assumes that a perfect image is modelled by a Gaussian histogram with μ mean and σ^2 variance, and the weight of each pixel is the back–projected probability of its intensity given the named Gaussian.

We will assume the same procedure of computing the weights with some small adjustments: while in (Mertens et al., 2007) for well-exposedness both outliers were weighted symmetrically, we favor darker tones to compensate the tendency of LIP models to favor bright tones, caused by their closing property. Details about the precise implementation parameters values will be provided in Section 5.

5. Implementation and evaluation procedure

We have implemented the HDR range algorithm described mainly by equation (8) within the LTIP model and weights similar to the procedure described in (Mertens et al., 2007) in Matlab. The actual values of the weights are standard for contrast $w_C = 1$, saturation $w_S = 1$, but differ for well-exposedness, where the mid range (Gaussian parameters) are $\mu = 0.37$ and $\sigma^2 = 0.2$. The choice will be further explained in section 6.

An example of achieved extended dynamic range may be seen in figure 3.

The common practice is to evaluate HDR methods using few publicly available images. We adopted the same principle, using more extensive public imagery data, such as the ones from (Čadík et al., 2008), OpenCV examples library and (Drago et al., 2003). We have evaluated the proposed algorithm on a database containing 22 sets of HDR frames acquired from various Internet sources, being constrained by the fact that the proposed method requires also the original frames and not only the HDR image. We made public[1] the full results and the code to obtain them so to encourage other people to further test it.

For the evaluation of the actual results, two category of methods are at hand: subjective evaluation and evaluation based on objective metrics.

5.1. Objective Evaluation

While not unanimously accepted, several metrics were created for the evaluation of TMOs in particular and HDR images in general. Here we will refer to the metrics introduced in (Aydin et al., 2008) and respectively the more recent one from (Yeganeh and Wang, 2013).

The metric from (Aydin et al., 2008), entitled "Dynamic Range (In)dependent Image Metrics" (DRIM) uses a specific model of the HVS to construct a virtual LDR image from the reference, given the HDR image and compares the contrast of the subject LDR image to the virtual one by considering three categories: artificial amplification of contrast, artificial loss of contrast and reversal of contrast. The metric points to pixels that are different to their standard perception according to the authors aforethought HVS modelling and a typical monitor setting ($\gamma = 2.2$, 30 pixels per degree and viewing distance of 0.5m). For each test image we normalized the error image by the original image size (as described in (Ferradans et al., 2012)). The metric only assigns one type of error (the predominant one) and has two shortcomings: it heavily penalizes global amplification error (which is not so disturbing from a subjective point of view) and it merely penalizes artifacts (such as areas with completely wrong luminance), which, for a normal viewer, are extremely annoying. Thus the metric, in fact assigns a degree of *perceptualness* (the sense of how close is that method to the human contrast transfer function) to a certain method.

A more robust procedure for evaluation was proposed in (Yeganeh and Wang, 2013) where, in fact, three scores were introduced:

- Structural fidelity which uses the structural similarity image metric (SSIM) (Wang et al., 2004) to establish differences between the LDR image and the original HDR one and a bank of non-linear filters based on the human contrast sensitivity function (CSF) (Barten, 1999). The metric points to structural artifacts of the LDR image with respect to the HDR image and has a 0.7912 correlation with subjective evaluation according to (Yeganeh and Wang, 2013).
- Statistical naturalness gives a score of the closeness of the image histogram to a normal distribution which was found to match average human opinion.
- Overall quality, Q which integrates the structural fidelity, S, and statistical naturalness, N, by :

$$Q = aS^{\alpha} + (1 - a)N^{\beta} \tag{9}$$

where $a = 0.8012$, $\alpha = 0.3046$, $\beta = 0.7088$ as found in (Yeganeh and Wang, 2013). The metric has 0.818 correlation with human opinion.

5.2. Subjective evaluation

On the subjective evaluation, for HDR images, Čadík et al. (Čadík et al., 2008) indicated the following criteria as

[1] The code and supplementary result are available at http://imag.pub.ro/common/staff/cflorea/cf_research.html/LIP.

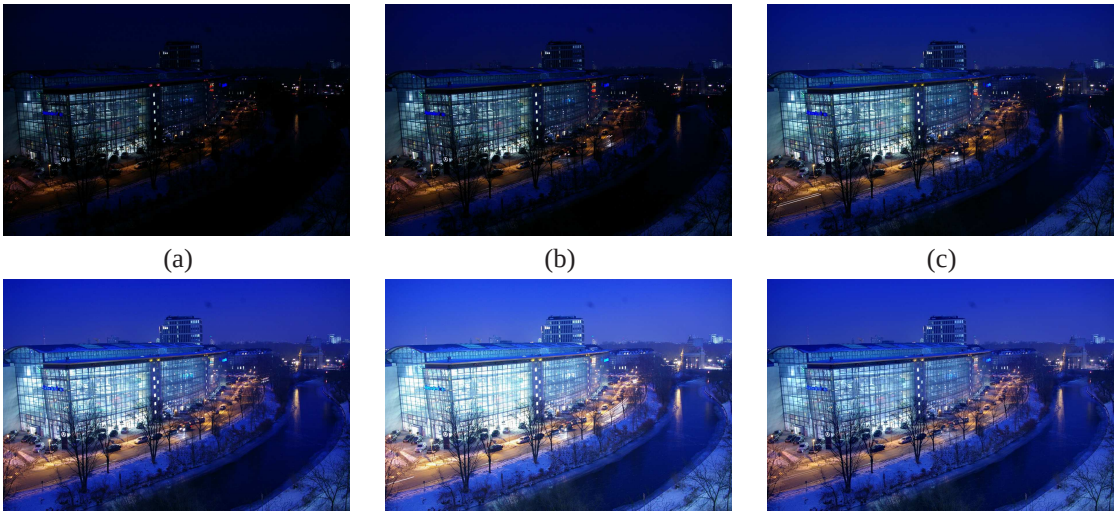

(a) (b) (c)

(d) (e) (f) HDR

Figure 3. Example of HDR imaging: initial, differently exposed frames (a-e)) and the HDR image obtained by using the proposed algorithm (f).

being relevant: luminosity, contrast, color and detail reproduction, and lack of image artifacts. The evaluation procedure was performed in two steps. First we analyze comparatively by means of example the overall appearance and existence of artifacts of the tested methods followed by intensive subjective evaluation.

To perform the actual evaluation we instructed 18 students in the 20-24 years range to examine and rank the images on their personal displays, taking into account the five named criteria. While we introduced them to a method for monitor calibration and discussed aspects about view angle and distance to monitor, we did not impose them as strict requirements since the average consumer do not follow rigorous criteria for visualization. Thus the subjective evaluation is more related to how pleasant and glistening an image is.

6. Results

6.1. Algorithm parameters

Logarithmic Model. The first choice of the proposed method is related to the specific Logarithm Image Processing model used. While we discuss this aspect by means of examples showed in figure 4, top row (b-d), we have to stres that all the results fall in the same line. The LTIP model provides the best contrast, while the classical LIP model (Jourlin and Pinoli, 1987) leads to very similar results, with marginal differences like slightly flatter sky and less contrast on the forrest. The symmetrical model (Patrascu and Buzuloiu, 2001) produces over–saturated images. Given the choice between the here solution and the one based on (Jourlin and Pinoli, 1987), as differences are rather small, the choice relies solely on the perceptual motivation detailed in section 4.

Next, given the parametric extension of the LTIP model from (Florea and Florea, 2013), we asked which is the best value for the parameter m. As showed in figure 4, bottom row (e-h), the best visual results are obtained for $m = 1$, which corresponds to the original LTIP model. Choices different from $m = 1$ use direct or inverse transformations that are too concave and, respectively, too convex, thus distorting the final results. Concluding, the best results are achieved with models that are closer to the human perception.

Algorithm weights. In section 4 we nominated three categories of weights (contrast – w_C, saturation w_S and well-exposedness) that interfere with the algorithm. For the first two categories, values different from standard ones ($w_C = 1$ and $w_S = 1$) have little impact.

The well-exposedness, which is described by mainly the central value μ of the ”mid range” has significant impact. As one can see in figure 5, the best result is achieved for $\mu = 0.37$ while for larger values ($\mu > 0.37$) the image is too bright and, respectively, for smaller ones ($\mu < 0.37$) is too dark. These findings were confirmed by objective testing, as further showed.

6.2. Comparison with state of the art

To test against various state of the art methods, we used the HDR irradiance map (stored as `.hdr` file) which was either delivered with the images (and typically produced using the method from (Robertson et al., 1999)), either pro-

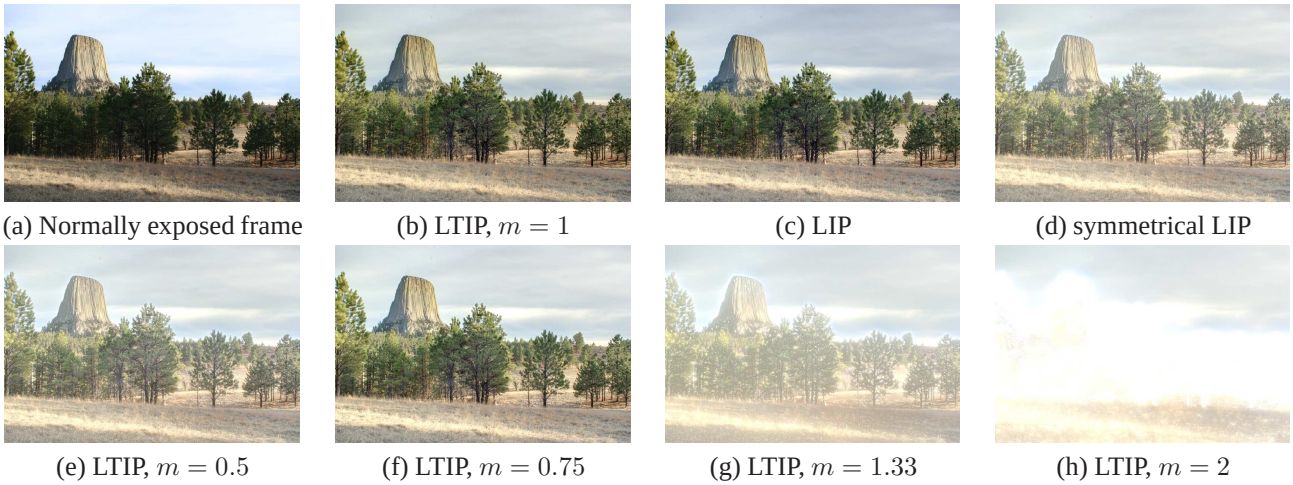

(a) Normally exposed frame (b) LTIP, $m = 1$ (c) LIP (d) symmetrical LIP

(e) LTIP, $m = 0.5$ (f) LTIP, $m = 0.75$ (g) LTIP, $m = 1.33$ (h) LTIP, $m = 2$

Figure 4. Normal exposed image frame (a) and the resulting image obtained by the standard LTIP model (b), Classical LIP model (c), symmetrical model introduced by Patrascu (d). Images obtained with the parametric extension of the LTIP model (e-h).

(a) $\mu = 0.32$ (b) $\mu = 0.37$ (c) $\mu = 0.4$ (d) $\mu = 0.5$

Figure 5. Output image when various values for mid-range (μ) in well-exposedness weight were used. The preferred choice is $\mu = 0.37$.

duced with some online available code[2].

For comparative results we considered the exposure fusion in the variant modified according to (Pece and Kautz, 2010) and the TMOs applied on the .hdr images described in (Ward et al., 1997), (Fattal et al., 2012), (Durand and Dorsey, 2002), (Drago et al., 2003), (Reinhard et al., 2005), (Krawczyk et al., 2005) and (Banterle et al., 2012) as they are the foremost such methods. The code for the last methods is taken from the Matlab HDR Toolbox that accompanies (Banterle et al., 2011) and is available online[3]. Note that envisaged TMO solutions include both global operators and local adaptation. A set of examples with the results produced with all the methods is in figure 6.

[2]The HDR creator package is available at `http://cybertron.cg.tu-berlin.de/pdci09/hdr_tonemapping/download.html`

[3]The HDR toolbox may be retrieved from `http://www.banterle.com/hdrbook/downloads/HDR_Toolbox_current.zip`

6.3. Objective metrics

Structure and Naturalness. We started the evaluation using the set of three objective metrics from (Yeganeh and Wang, 2013). The results obtained are presented in table 3. The best performing version of the proposed method was for $\mu = 0.37$ and it ranked first, according to the overall quality and statistical naturalness, and it rank fifth according to structural fidelity (after (Banterle et al., 2012), (Reinhard et al., 2005), (Drago et al., 2003) and (Durand and Dorsey, 2002)). Concluding, we consistently rank as top performing method, with the exception of structural similarity, where our method was penalized when compared to other TMO due to their general adaptation being closer to the standard contrast sensitivity function (CSF) (Barten, 1999).

Furthermore, the proposed method is the closest to the standard exposure fusion result (Mertens et al., 2007), which is currently the baseline method for photographer enthusiasts while building HDR images. This aspect is showed in table 4, where we computed the natural logarithm of the Root-Mean-Square to the image resulting from the standard exposure fusion and, respectively, the structural simi-

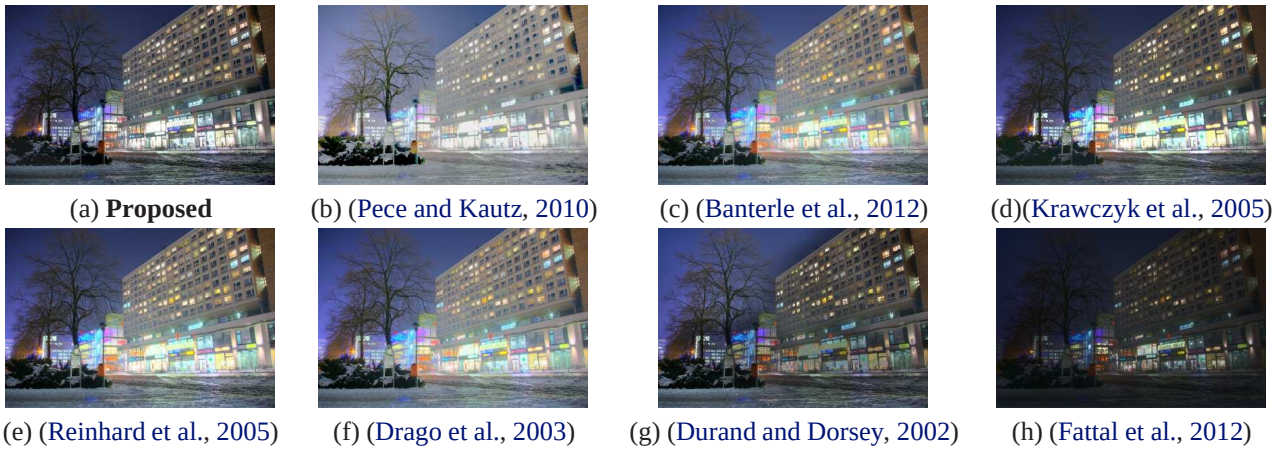

(a) **Proposed** (b) (Pece and Kautz, 2010) (c) (Banterle et al., 2012) (d)(Krawczyk et al., 2005)

(e) (Reinhard et al., 2005) (f) (Drago et al., 2003) (g) (Durand and Dorsey, 2002) (h) (Fattal et al., 2012)

Figure 6. The resulting images when various methods and, respectively, various state of the art tone mapping operators were used.

Table 3. HDR image evaluation by the average values for structural fidelity (S), statistical naturalness (N) and the overall quality (Q). With bold letters we marked the best result according to each category.

Method	S[%]	N[%]	Q[%]
(Ward et al., 1997)	66.9	14.38	72.7
(Fattal et al., 2012)	59.9	6.4	61.0
(Durand and Dorsey, 2002)	81.7	41.0	85.4
(Drago et al., 2003)	82.3	50.2	87.0
(Reinhard et al., 2005)	83.1	50.5	87.5
(Krawczyk et al., 2005)	71.7	36.8	76.6
(Banterle et al., 2012)	**83.7**	52.1	87.8
(Pece and Kautz, 2010)	74.7	22.4	79.2
Proposed, $\mu = 0.5$	81.0	39.2	84.5
Proposed, $\mu = 0.4$	81.6	52.1	87.3
Proposed, $\mu = 0.37$	81.5	**57.4**	**88.0**
Proposed, $\mu = 0.32$	81.4	53.7	87.4

larity when compared to the same image.

Perceptualness. One claim of the current paper is that the proposed method adds perceptualness to the exposure fusion. To test this, we compared our method against the standard exposure fusion, (Mertens et al., 2007) using the perceptual DRIM metric from (Aydin et al., 2008). Over the considered database, the proposed method produced an average total error (the sum of three categories) with 2 percent smaller than the standard exposure fusion (64.5% compared to 66.8%). On individual categories, the proposed method produced a smaller amount of amplification of contrast, with comparable results on loss and reversal of contrast. Thus, overall, the results confirm the claim.

Table 4. HDR image evaluation by taking the log of root mean square to standard exposure fusion. Best values are marked with bold letters.

Method	logRMSE[dB]	SSIM
(Ward et al., 1997)	149.9	83.5
(Fattal et al., 2012)	281.1	38.1
(Durand and Dorsey, 2002)	160.5	74.4
(Drago et al., 2003)	148.4	74.7
(Reinhard et al., 2005)	148.4	74.8
(Krawczyk et al., 2005)	136.9	66.4
(Banterle et al., 2012)	147.9	75.2
(Pece and Kautz, 2010)	196.3	65.2
Proposed	**72.1**	**93.8**

6.4. Artifacts

The HDR-specific objective metrics have the disadvantage of not properly weighting the artifacts that appear in images, while human observers are very disturbed by them. This fact was also pointed by (Čadík et al., 2008) and to compensate we performed visual inspection to identify disturbing artifacts. The proposed method never produced any artifact. Examples of state of the art methods and artifact produced may be seen in figure 7.

In direct visual inspection, when compared against the standard exposure fusion method (Mertens et al., 2007), our algorithm shows details in bright areas, while normal, real–based operation do not. This accretion is due to the closing property of the logarithmic addition and respectively scalar amplification. This aspect is also visible when comparing with the most robust TMO based method, namely (Banterle et al., 2011). Examples that illustrate these facts are presented in figure 8.

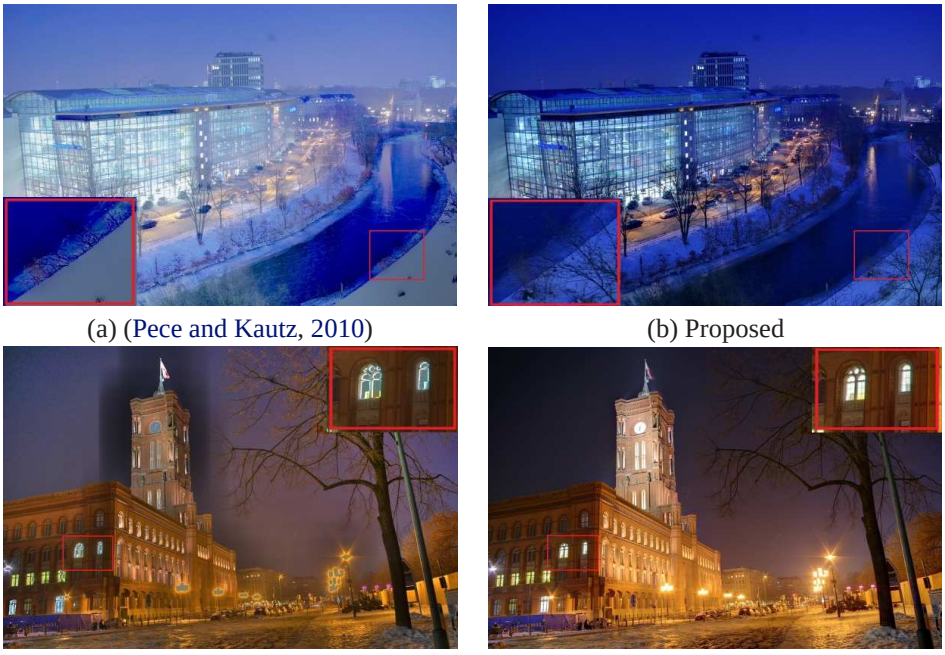

(a) (Pece and Kautz, 2010) (b) Proposed

(c) (Durand and Dorsey, 2002) (d) Proposed

Figure 7. Examples of artifacts produced by state of the art methods compared to the robustness of the proposed method. Close-ups point to artifact areas.

6.5. Mean Opinion Score

Regarding the results of the multiple non-expert subjective evaluation, the proposed method was selected as the best one by 10 users, the exposure fusion (Mertens et al., 2007) by 7, while in the rest of the methods won in 1 case. Also the second place was monopolized by the ”glossier” exposure fusion based methods.

When compared to direct exposure fusion proposed by (Mertens et al., 2007), due to the perceptual nature of the proposed method, a higher percentage of the scene dynamic range is in the visible domain; direct fusion losses information in the dark-tones domain and respectively in very bright part; thus the narrow margin for our method win.

7. Discussion and Conclusions

In this paper we shown that the LTIP model is compatible with the Naka-Rushton equation modelling the light absorption in the human eye and similar with the CRF of digital cameras. Upon these findings, we asserted that it is possible to treat different approaches to HDR imaging unitary. Implementation of the weighted sum of input frames is both characteristic to irradiance map fusion and to exposure fusion. If implemented using LTIP operations, the perceptualness is added to the more popular exposure fusion. Finally, we introduced a new HDR imaging technique that adapts the standard exposure fusion to the logarithmic type operations, leading to an algorithm which is consistent in both theoretical and practical aspects. The closing property of the LTIP operations ensures that details are visible even in areas with high luminosity, as previously showed.

The method maintains the simplicity of implementation typical to the exposure fusion, since the principal difference is the redefinition of the standard operations and different parameter values. The supplemental calculus associated with the non-linearity of LTIP operation could easily be trimmed out by the use of look-up tables, as showed in (Florea and Florea, 2013).

The evaluation results re-affirmed that in an objective assessment aiming at naturalness and pleasantness of the image, the proposed method outperforms irradiance map fusion followed by TMOs as they try to mimic more a theoretical model which is not perfect and is not how the normal user expects HDR images to be. The same conclusion was emphasized by the subjective evaluation, where methods developed in the image domain are preferred as the resulting images are more ”glistening”. The proposed method, having a psychovisual inspired global adaptation and ”glossy” tuned local adaptation, ranks best in the subjective evaluation even by a narrow margin.

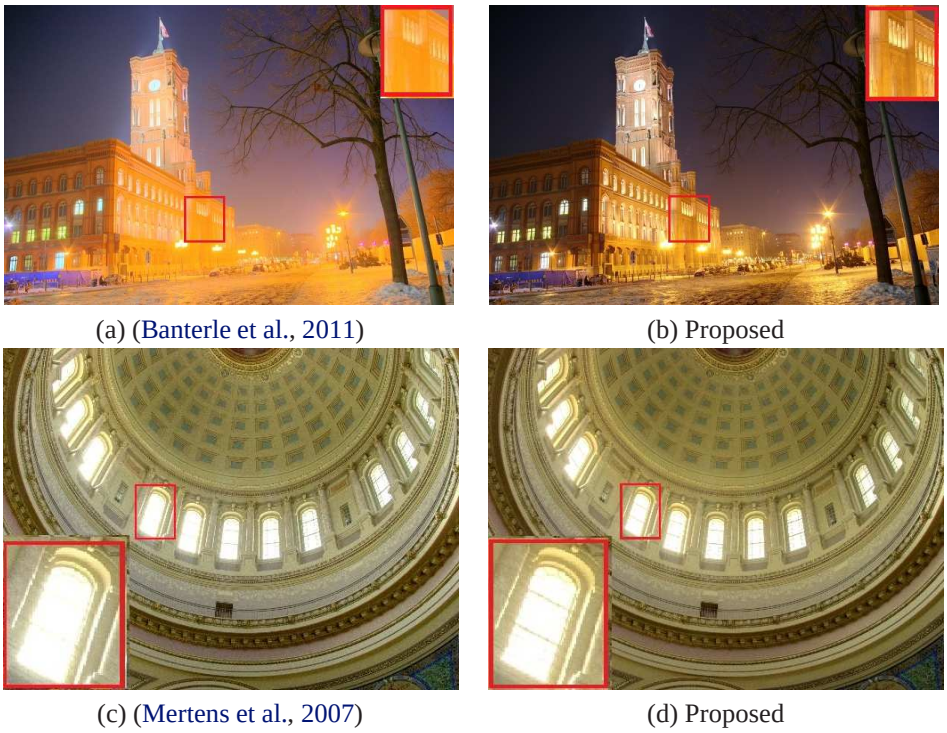

(a) (Banterle et al., 2011) (b) Proposed

(c) (Mertens et al., 2007) (d) Proposed

Figure 8. Examples of loss of details produced by state of the art methods compared to the robustness of the proposed method.

Acknowledgments

The authors wish to thank Martin Cadik for providing the frames for testing. We also would like to thank Tudor Iorga for running tests and providing valuable ideas. The work has been partially funded by the Sectoral Operational Programme Human Resources Development 2007-2013 of the Ministry of European Funds through the Financial Agreement POSDRU/159/1.5/S/134398.

References

Aydin, T., Mantiuk, R., Myszkowski, K. and Seidel, H. (2008). Dynamic range independent image quality assessment, *ACM Transactions on Graphics (TOG)*, Vol. 27(3), pp. 1–10.

Banterle, F., Artusi, A., Debattista, K. and Chalmers, A. (2011). *Advanced High Dynamic Range Imaging: Theory and Practice*, AK Peters (CRC Press), Natick, MA, USA.

Banterle, F., Artusi, A., Sikudova, E., Edward, T., Bashford-Rogers, W., Ledda, P., Bloj, M. and Chalmers, A. (2012). Dynamic range compression by differential zone mapping based on psychophysical experiments, *ACM Symposium on Applied Perception (SAP)*, pp. 39–46.

Barten, P. G. J. (1999). *Contrast Sensitivity of the Human Eye and Its Effects on Image Quality*, SPIE, Washington, DC.

Čadík, M., Wimmer, M., Neumann, L. and Artusi, A. (2008). Evaluation of HDR tone mapping methods using essential perceptual attributes, *Computers & Graphics* **32(3)**: 330–349.

Debevec, P. and Malik, J. (1997). Recovering high dynamic range radiance maps from photographs, *ACM SIGGRAPH*, pp. 369–378.

Deng, G., Cahill, L. W. and Tobin, G. R. (1995). A study of logarithmic image processing model and its application to image enhancement, *IEEE Transactions on Image Processing* **4(4)**: 506 – 512.

Drago, F., Myszkowski, K., Annen, T. and Chiba, N. (2003). Adaptive logarithmic mapping for displaying high contrast scenes, *Computer Graphics Forum* **22(3)**: 419 – 426.

Durand, F. and Dorsey, J. (2002). Fast bilateral filtering for the display of high-dynamic-range images, *ACM Transactions on Graphics* **21(3)**: 257 – 266.

Fattal, R., Lischinski, D. and Werman, M. (2012). Gradient domain high dynamic range compression, *ACM Transactions on Graphics (TOG)* **21(3)**: 249–256.

Ferradans, S., Bertalmio, M., Provenzi, E. and Caselles, V. (2012). An analysis of visual adaptation and contrast perception for tone mapping, *IEEE Transactions on Pattern Analysis and Machine Intelligence* **33(10)**: 2002–2012.

Florea, C. and Florea, L. (2013). Parametric logarithmic type image processing for contrast based auto-focus in extreme lighting conditions, *International Journal of Applied Mathematics and Computer Science* **23(3)**: 637 – 648.

Gilchrist, A., Kossyfidis, C., Bonato, F., Agostini, T., Cataliotti, J., Li, X., Spehar, B., Annan, V. and Economou, E. (1999). An anchoring theory of lightness perception, *Psychological Review* **106**(4): 795–834.

Grossberg, M. D. and Nayar, S. K. (2004). Modeling the space of camera response functions, *IEEE Transactions on Pattern Analysis and Machine Intelligence* **26 (10)**: 1272 – 1282.

Jourlin, M. and Pinoli, J. C. (1987). Logarithmic image processing, *Acta Stereologica* **6**: 651 – 656.

Krawczyk, G., Myszkowski, K. and Seidel, H.-P. (2005). Lightness perception in tone reproduction for high dynamic range images, *Computer Graphics Forum*, Vol. 24, pp. 635–645.

Macmillan, N. and Creelman, C. (eds) (2005). *Detection theory and: A user's guide*, Lawrence Erlbaum.

Mann, S. and Mann, R. (2001). Quantigraphic imaging: Estimating the camera response and exposures from differently exposed images, *Porc. of IEEE Computer Vision and Pattern Recognition*, Vol. 1, pp. 842–849.

Mann, S. and Picard, R. (1995). Being 'undigital' with digital cameras: Extending dynamic range by combining differently exposed pictures, *Proceedings of IS&Ts 48th Annual Conference*, Vol. 1, pp. 422–428.

Mertens, T., Kautz, J. and Reeth, F. V. (2007). Exposure fusion, *Proceedings of Pacific Graphics*, pp. 382 – 390.

Meylan, L., Alleysson, D. and Susstrunk, S. (2007). Model of retinal local adaptation for the tone mapping of color filter array images, *Journal of Optical society of America, A* **24**: 2807 – 2816.

Mitsunaga, T. and Nayar, S. K. (1999). Radiometric self calibration, *Proceedings of IEEE Conference on Computer Vision and Pattern Recognition*, Vol. 1, pp. 374–380.

Naka, K.-I. and Rushton, W. A. H. (1966). S-potentials from luminosity units in the retina of fish (cyprinidae), *The Journal of Physiology* **185**: 587 – 599.

Navarro, L., Courbebaisse, G. and Deng, G. (2013). The symmetric logarithmic image processing model, *Digital Signal Processing* **23(5)**: 1337 – 1343.

Panetta, K., Zhou, Y., Agaian, S. and Wharton, E. (2011). Parameterized logarithmic framework for image enhancement, *IEEE Transactions on Systems, Man, and Cybernetics - part B: Cybernetics* **41**(2): 460 – 472.

Patrascu, V. and Buzuloiu, V. (2001). Color image enhancement in the framework of logarithmic models, *Proceedings of the 8th IEEE International Conference on Telecommunications*, Vol. 1, Bucharest, Romania, pp. 199 – 204.

Pece, F. and Kautz, J. (2010). Bitmap movement detection: Hdr for dynamic scenes, *Proceedings of Conference on Visual Media Production*, pp. 1–8.

Pinoli, J. C. and Debayle, J. (2007). Logarithmic adaptive neighborhood image processing (LANIP): Introduction, connections to human brightness perception, and application issues, *EURASIP Journal on Advances in Signal Processing* **1**: 114–114.

Rafajlowicz, E., Pawlak, M. and Steland, A. (2005). Nonlinear image processing and filtering: A unified approach based on vertically weighted regression, *International Journal of Applied Mathematics and Computer Science* **18**(1): 49 – 61.

Reinhard, E., Stark, M., Shirley, P. and Ferwerda, J. (2002). Photographic tone reproduction for digital images, *ACM Transactions on Graphics* **21**: 267–276.

Reinhard, E., Ward, G., Pattanaik, S. and Debevec, P. (2005). *High Dynamic Range Imaging: Acquisition, Display and Image-Based Lighting*, Morgan Kaufmann Publishers, San Francisco, California, S.U.A.

Robertson, M., Borman, S. and Stevenson, R. (1999). Dynamic range improvement through multiple exposures, *Proceedings of International Conference on Image Processing*, pp. 159 – 163.

Stevens, J. and Stevens, S. (1963). Brightness functions: Effects of adaptation, *Jorunal of Optical Society of America A* **53**: 375–385.

Stevens, S. (1961). To honor Fechner and repeal his law, *Science* **133**: 80–133.

Tamburino, D., Alleysson, D., Meylan, L. and Strusstruk, S. (2008). Digital camera workflow for high dynamic range images using a model of retinal process, *Proceedings of SPIE*, Vol. 6817.

Valeton, J. and van Norren, D. (1983). Light adaptation of primate cones: an analysis based on extracellular data, *Vision Research* **23(12)**: 1539 – 1547.

Vertan, C., Oprea, A., Florea, C. and Florea, L. (2008). A pseudo-logarithmic framework for edge detection, *Advanced Concepts for Intelligent Vision Systems*, Vol. 5259, pp. 637 – 644.

Wang, Z., Bovik, A. C., Sheikh, H. R. and Simoncelli, E. P. (2004). Image quality assessment: From error visibility to structural similarity, *IEEE Transactios on Image Processing* **13(4)**: 600–612.

Ward, G., Rushmeier, H. and Piatko, C. (1997). A visibility matching tone reproduction operator for high dynamic range scenes, *IEEE Transactions on Visualization and Computer Graphics* **3**: 291–306.

Yeganeh, H. and Wang, Z. (2013). Objective quality assessment of tone mapped images, *IEEE Transactios on Image Processing* **22(2)**: 657–667.

8. Biographies

Corneliu Florea was born in 1980 in Bucharest. He got his master degree from University "Politehnica" of Bucharest in 2004 and the PhD from the same university in 2009. There, he lectures on statistical signal and image processing, and has introductory courses in computational photography and computer vision. His research interests include non-linear image processing algorithms for digital still cameras and computer vision methods for portrait understanding. He is author of more than 30 peer-reviewed papers and of 20 US patents and patent applications.

Constantin Vertan Professor Constantin Vertan holds an image processing and analysis tenure at the Image Processing and Analysis Laboratory (LAPI) from the Faculty of Electronics, Telecommunications and Information Technology at the Politehnica University of Bucharest. He was an invited professor at INSA de Rouen and University of Poitiers (France). For his contributions in image processing he was awarded with UPB "In tempore opportuno" award (2002), Romanian Reaserch Council "In hoc signo vinces" award (2004) and was promoted as IEEE Senior Member (2008). His research interests are general image processing and analysis, content-based image retrieval, fuzzy and medical image processing applications and authored more than 50 peer-reviewed papers. He is the secretary of the Romanian IEEE Signal Processing Chapter and associate editor at EURASIP Journal on Image and Video Processing.

Laura Florea received her PhD in 2009 and M.Sc in 2004 from University "Politehnica" of Bucharest. From 2004 she teaches classes in the same university, where she is currently a Lecturer. Her interests include image processing algorithms for digital still cameras, automatic understanding of human behavior by analysis of portrait images, medical image processing and statistic signal processing theory. Previously she worked on computer aid diagnosis for hip joint replacement. She is author of more than 30 peer-reviewed journal and conference papers.